ORIGINAL RESEARCH ARTICLE
UHD JOURNAL OF SCIENCE AND TECHNOLOGY

An Effective Computer-aided diagnosis Technique for Alzheimer's Disease Classification using U-net-based Deep Learning

Fawzi Abdul Azeez Salih[1], Shaniar Tahir Mohammed[2], Tofiq Ahmed Tofiq[2], Hataw Jalal Mohammed[3]

[1]Department of Computer Science, College of Basic Education, University of Sulaimani, Sulaimani, Iraq, [2]Department of Computer Science, College of Science, University of Sulaimani, Sulaimani, Iraq, [3]Charmo Center for Research, Training, and Consultancy, University of Charmo, Sulaimani, Iraq

ABSTRACT

The diagnosis of Alzheimer's disease (AD), a common neurodegenerative disease that impairs thinking and memory abilities in older adults and ultimately results in cognitive impairment and dementia, is made possible in large part by computer-aided diagnosis (CAD). The idea has been to use either machine learning models or deep learning models to develop classification techniques for this disease. CAD techniques and mechanisms have emerged to help and facilitate early detection of this disease as a fundamental step in its treatment plan. As part of our approach, we proposed a model that included the following two pre-processing steps: Contrast Limited Adaptive Histogram Equalization (CLAHE) was utilized to enhance image contrast, especially in low-contrast areas. Normalization was then incorporated to ensure reliable training and faster convergence. A Gray-level co-occurrence matrix technique was used to extract seven texture features from the images following pre-processing: contrast, homogeneity, energy, correlation, variance, dissimilarity, and entropy. After that, these characteristics were added to the model output before the last classification layer. The best hybrid framework out of the five models we examined in this paper was utilized to build a convolutional neural network that can be used to identify AD characteristics from magnetic resonance images. As discussed in Section IV of this article, the U-Net model was selected because of its superior performance. The experimental results demonstrate that this technique showed great accuracy in segmentation and classification for each of the five AD Neuroimaging Initiative categories when a specific diagnosis was made. These results are as follows: Overall, the five classes' final average scores for the four measures were as follows: 94.46% for Accuracy, 94.32% for Precision, 94.49% for Recall, and 94.41% for F1-score.

Index Terms: Alzheimer Diseases, CLAHE, U-Net, Convolutional Neural Network, Magnetic Resonance Imaging, Alzheimer's Disease Neuroimaging Initiative

1. INTRODUCTION

Today, due to the advancements in the fields of biomedical engineering, data acquisition techniques, and data analytics, Computer-aided diagnosis (CAD) systems are used across almost all the fields of medicine [1], and one of the prevalent diseases in medicine fields is the progressive neurodegenerative disorder brain atrophy Alzheimer's disease (AD) [2], which is characterized as a most common neurological disorder that ultimately triggers an irreversible decline in cognitive function sciences [3], because it is a very multifaceted ailment that reasons brain disappointment, then ultimately, dementia ensues. It is a global health problem. (99%) of clinical trials have failed to limit the progression

Access this article online

DOI: 10.21928/uhdjst.v9n1y2025.pp34-43	E-ISSN: 2521-4217 P-ISSN: 2521-4209

Corresponding author's e-mail: Fawzi Abdul Azeez Salih, Department of Computer Science, College of Basic Education, University of Sulaimani, Sulaimani, Iraq. E-mail: fawzi.barznji@univsul.edu.iq

Received: 10-01-2025 Accepted: 09-02-2025 Published: 25-02-2025

of it [1]. The calculated annual fee of dementia is predicted to be a trillion US dollars and is predicted to double by 2030 [4]. According to the World Health Organization (WHO) report, more than 55 million people suffer from dementia worldwide, and more than (60%) of them live in low- and middle-income and learning countries. Every year, there are approximately 10 million new cases [5], and by 2050, it is expected to reach 13.8 million [4]. This indicates that the prevalence of this disease will increase by more than (200%) over the next 15 years [6].

As illustrated in Fig. 1, AD has five stages: (1) AD dementia with severe symptoms, then (2) Late Mild Cognitive Impairment (LMCI), (3) Mild Cognitive Impairment (MCI): which is a condition that precedes dementia but does not meet the criteria for a diagnosis of AD, (4) Early Mild Cognitive Impairment (EMCI), (5) Cognitively Normal (CN): pre-clinical dementia, which is classified by the symptom-free period that occurs between the initial brain lesions and the onset of the first symptoms [7].

The indications of AD typically evolve slowly and gradually, and also patients may show various symptoms at cognitive and behavioral levels; therefore, it can be difficult and complex to diagnose AD. Within this framework, developing innovative diagnostic tools to help diagnosing the disease at an earlier stage is a challenging task. In this context, there has been growing interest in using CAD systems for automatic detection of AD [8]. A variety of CAD approaches have been proposed for the early diagnosis of various stages of AD using Magnetic resonance imaging (MRI) [9], recently provided a non-invasive imaging approach that can detect subtle morphological changes in the brain [3]. MRI-based atrophy measurements are considered valid markers of disease state and progression since atrophy seems to be an inevitable and intrinsic factor of progressive neurodegeneration. Moreover, changes in structural measures, such as ventricular enlargement, entorhinal cortex, whole brain, and temporal lobe volumes, can be associated with modifications in cognitive performance [7]. MRI scans provide detailed insights into blood circulation and cerebral processes. Still, they cannot detect brainwave activity or facilitate communication between tumor cells [8], in addition, dissimilar X-rays, MRI does not emit ionizing radiation, so it can be considered a valuable opportunity to track the development of AD and monitor the effectiveness of treatment [10]. With the development of artificial intelligence (AI) and the great progress in the field of computer vision and deep learning (DL) over the past years, CAD applications in the medical field have become widespread and play an important role in diagnosing diseases, including the subject of our research (AD) [11]. In CAD systems, DL is now making great strides in medical image analysis [12]. DL has increased importance in medical image analysis, driving the pursuit of AI in medical imaging, which is widely accepted for pattern recognition, primarily due to their unique feature of being trainable as a complete program [8]. A huge number of articles and researches have been published through the internet about attendance and the importance of DL in medical images, these ideas and approaches have included individually or mixed (characterization, detection, segmentation, registration, and classification). In the field of medical imaging, especially in the analysis of AD, there is a well-known trend of merging DL models with node segmentation models include several network architectures, such as convolutional neural network (CNN), which are the furthermost used, VGG16, ResNet, U-Net, Mask R-CNN, etc. [13]. The human brain has a structure with many unique features that can be extracted by different CNN models [14]. U-net is one of the greatest prevalent network constructions used typically for segmentation [15], because it is a semantic segmentation network that is constructed on the full CNN, and was sophisticated in 2015 for the processing of medical images [16]. Instead of using single pixels to diagnose disorders, such as Alzheimer's, trends across regions of interest must be analyzed. Pixel-level image quality should be strong, with enough contrast and

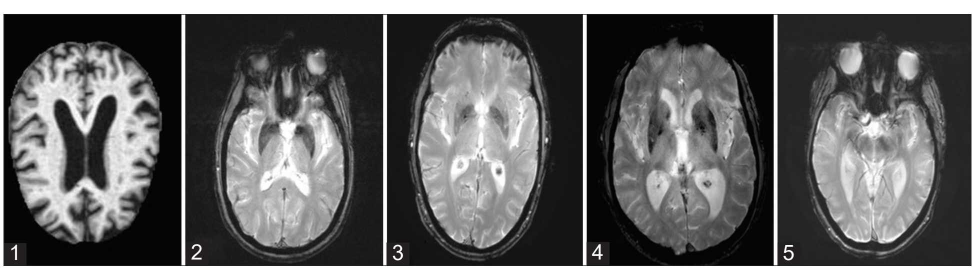

Fig. 1. Samples of magnetic resonance imaging images representing different Alzheimer's disease (AD) stages. (1) AD, (2) Late mild cognitive impairment; (3) Mild cognitive impairment, (4) Early mild cognitive impairment, (5) Cognitively normal.

spatial resolution to reliably identify diseased or anatomical characteristics. The study's minimal pixel quality should be in line with the requirements of the imaging modality. Pixels of poor quality may produce noise or artifacts that jeopardize the diagnostic results and model reliability. Along with advancing quality control measures, these permits employing the measurable features of impairment (area, direction, etc.). This also makes it probable to well understand the tincture of impairment and develop phases to disregard it. To realize this, the U-Net neural network offers for the semantic segmentation of images, where each image pixel is classified as belonging to one of the damaged classes, or to the undamaged part.

2. RELATED WORK

In this part of our article, we will try to provide a comprehensive review of the articles conducted during the past 5 years that is similar to the same topic of our study. Xia *et al.* 2020 [17], proposed a new combined CNN framework for AD detection, and mutually 3D CNN and 3D convolutional long short-term memory (3D CLSTM) were used. They exploit a 3D CNN consist of 6 layers to learn instructive features first, then 3D CLSTM is increased to additional extract the channel-wise higher-level information. The model applied on AD Neuroimaging Initiative (ADNI) dataset and achieved (94.19%) of accuracy rate. Murugan *et al.*, in 2021 [18], employed a DEMentia NETwork (DEMNET) with CNN to extract the discriminative features contained (4) core phases: pre-processing data, balancing dataset consuming Synthetic Minority Over-sampling Technique (SMOTE), Splitting dataset, and classification using DEMNET to detect the dementia stages from MRI obtained from Kaggle using the ADNI dataset to predict AD classes. The proposed DEMNET achieved an accuracy of (95.23%) and an area under curve of (97%). Zhu *et al.* also in 2021 [19], proposed a Patch-Net to generate local illustrations from the brain MRIs. They developed an attention-based pooling block for features mixture and completely -associated layers assisted for final calculations. Their model investigated on ADNI dataset, and they obtained the best result was (92.40%) of accuracy rate. Furthermore, in 2021, Shoaip *et al.* [20], used the ADNI dataset and aimed to propose an interpretable approach to detect AD based on AD diagnosis ontology and the expression of semantic web rule language, by applying an ontology-based method that employs (3) diverse machine learning algorithms, such as random forest, JRip, and J48, after excluding features with a high percentage of missing data, such as DIGITSCOR, AV45, ABETA, TAU, and EcogSPTotal. The proposed classifiers achieved an accuracy of (94.1%) and a precision of (94.3%). Helal *et al.* in 2022, used the ADNI Medical Image dataset and proposed a main objective framework with DL-AD (DL-AHS) based on the U-Net architecture and estimated using the Processing, Analysis, and Visualization technique. They anticipated two architectures for left and right HC segmentation from other brain sub-regions. First utilized simple hyperparameters tuning in the U-Net (SHPT-Net) and the second employed a transfer learning technique in which the ResNet blocks are used in the U-Net (RESU-Net). The result achieved a performance (94.34%) of accuracy rate [21]. In 2023, Noh *et al.* [22], employed spatial and sequential feature extractors, utilized the former U-Net construction in extraction, after that used LSTM to extract temporal features, and executed (4)-step pre-processing to eliminate noise from the fMRI images. In their trained approach, they qualified each of the (3) models by fine-tuning the time measurement. Finally, they revealed an average (96.4%) of accuracy when consuming (5)-fold cross-validation. Furthermore, in 2023, Chen *et al.* [23], proposed a model that directly modeled the brain's organizational networks from DTI. They linked the permanent toolkits, Brain Diffuser, and thwarted additional operational connectivity features and disease-related information by investigating differences in structural brain networks across subjects. They achieved an accuracy rate of (87.83%), Precision (87.83%), Recall (92.66), and F1-score (87.83). In the same year, Bhosale *et al.* 2023 [24], used a U-Net Convolutional Network-based approach to segment AD from ADNI 2D brain MRI images. By implementing a series of convolutional functions using a (3 × 3) filter as the initial design of the U-Net, they used a mixing technique of minimum pooling and average pooling as a hybrid pooling instead of using only maximum pooling. Finally, their updated approach clearly outperformed the original U-Net model, achieving an impressive performance of (91.23%) accuracy. Gupta *et al.* in 2024 [2], conducted an organized evaluation to investigate the estimation of AD on existing toolkits in the ADNI dataset using the Preferred Reporting Item for Systematic Review and Meta-Analysis strategies using ADNI dataset and presented AD Detection Network employment, They achieved results: an accuracy rate of (94.33%), Precision (90.4%), Recall (90.3%) and F1-Score (91.2%). Firdos *et al.* in 2024 [25], explored the effectiveness of CNN constructions, such as UNet, LeNet, and GoogLeNet, and revealed that the CNN model achieved the highest accuracy, with LeNet achieved an accuracy of (97%), UNet at (94%), and GoogLeNet at (51%), using ADNI dataset images. These focus attention on the potential of DL to improve the detection and classification of AD and prepare early

TABLE 1: Summary of related works (They all used the ADNI dataset)

Related work	Preprocessing	Model training	Feature extraction	Classification	Results
Xia *et al*. 2020 [17]	Not detailed	3D CLSTM	Spatial information from the 3D	3D CNN and 3D CLSTM	Accuracy 94.19%
Murugan *et al*., [18]	Spatial rotation, flipping, scaling,	DEMNET	Spatial features.	softmax activation function	Accuracy 95.23% AUC 97%.
Zhu *et al*. [19]	Skull stripping, spatial normalization, and intensity normalization	Dual Attention Multi-Instance Deep Learning (DA-MIDL)	Deep features from each 3D patch	Fully connected layer followed by a softmax activation function	Accuracy 92.40%
Shoaip *et al*. [20]	Skull stripping, intensity normalization, and spatial alignment	Semantic rule-based framework.	Brain volume metrics (e.g., hippocampus, entorhinal cortex)	Semantic reasoning engine	Accuracy 94.1% and precision 94.3%
Helal *et al*. [21]	Skull stripping, spatial normalization, and intensity normalization	Neural Network: U-Net-like architecture	Hippocampus and cortical regions	InceptionV3-TL	Accuracy 94.34%
Noh *et al*. [22]	Motion correction, Slice timing correction, Spatial normalization, Spatial smoothing. Region of Interest (ROI)	Support Vector Machine (SVM)	3D-CNN used to extract spatial features and the rs-fMRI for temporal	Utilization of SVM to classify subjects into respective categories	Accuracy 96.4%
Chen *et al*. [23]	Noise reduction and tensor reconstruction. Spatial alignment. Extraction of fractional anisotropy (FA) and mean diffusivity (MD).	A novel diffusion-based generative model called "Brain Diffuser"	Feature Extraction Net (FENet) to extract the structural attributes from DTI.	Neural network models integrated into the pipeline for disease classification	Accuracy 87.83% Precision 87.83% Recall 92.66% F1-score 87.83%
Bhosale *et al*. [24]	Noise reduction, Normalization, Skull stripping, Resizing.	Enhanced U-Net architecture	Gray matter, white matter, cerebrospinal fluid, Volumetric features.	A shallow neural network trained on extracted features.	Accuracy 91.23%
Gupta *et al*. [2]	Image Registration, Normalization, Skull Stripping	Adversarial Network-based architecture designed for multimodal data	sMRI: gray matter volume, cortical thickness, and hippocampal shape. fMRI: Captured functional connectivity patterns and brain activity networks.	Dense neural network	Accuracy 94.33% Precision 90.4% Recall 90.3% F1-score 91.2%
Firdos *et al*. in 2024 [25]	Resizing: dimensions required by GoogLeNet, LeNet, and UNet. Normalization. Data Augmentation: rotations, flips, and brightness. Segmentation (UNet-specific).	GoogLeNet LeNet UNet	GoogLeNet: multi-scale spatial features. LeNet: Captured basic structural patterns. UNet: Focused on segmenting brain regions.	Effectiveness of CNN constructions, such as UNet, LeNet, and GoogLeNet	Accuracy GoogLeNet 51% LeNet 97% UNet at 94%

AUC: Area under curve, CNN: Convolutional neural network, ADNI: Alzheimer's disease Neuroimaging Initiative

interferences and individual care effortless. The promising results from the CNN model's highpoint, their ability to convert the clinical technique to Alzheimer's, highlighting the importance of technical developments in addressing this incapacitating state. Table 1 below summarizes the related works, and describes (Dataset, Pre-processing, model training, feature extraction, classification, and results).

3. PROPOSED METHOD

In this study, we proposed a hybrid image classification approach (U-Net CNN) to classify the five pre-determined classes of AD. The method was divided into several stages: image pre-processing, feature extraction, and DL-based classifications as shown in Fig. 2 below.

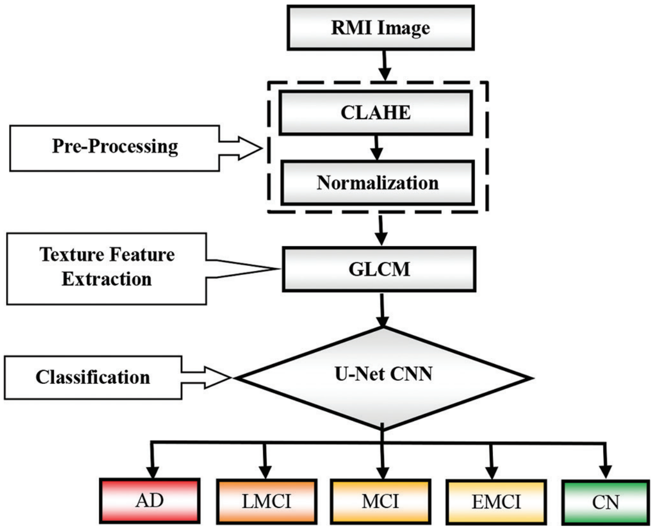

Fig. 2. The block diagram of the proposed approach.

3.1. Pre-Processing

To reduce the (time requested and the learning difficulty) of the proposed model, we increased the contrast level of the images and then we normalized them which is very necessary for detecting and classification of AD cases. This pre-processing stage included two steps:

a. Using contrast limited adaptive histogram equalization (CLAHE) which performed to enhance the contrast of specific ranges by adjusting the intensity levels according to local histograms [26], as shown in Fig. 3. This leads to additional detailed illustration of the crucial structural features of and improve our technique.

b. There are several types of normalization, such as intensity normalization (IN), spatial normalization, Z-score normalization, and numerical normalization. That can be used to remove some variations in the data, such as different subject pose or differences in image contrast, to simplify the detection of subtle differences [21]. In our proposed model, IN was used, where the pixel intensity values of the images are normalized to the range [0, 1] by dividing the pixel values by 255. This kind of normalization confirms that the input data has steady intensity levels, refining convergence throughout training and making the model fewer sensitive to variations in input brightness. Fig. 4 illustrates the result of normalizing on the same images that used in Fig. 3.

3.2. Texture Feature Extraction

Enables the extraction of valuable information for tasks, such as texture classification and segmentation [27]. Everywhere, when the Gray-level co-occurrence matrix (GLCM) is computed, there are seven numerous statistical measures (Contrast, Homogeneity, Energy, Correlation, Variance, Dissimilarity, and Entropy) can be derived from it to characterize the texture and structure of the image. Experimenting with different parameters and features allows for fine-tuning the analysis to specific application requirements, making GLCM a versatile tool in the field of image processing and computer vision [27].

3.3. U-net-based DL Framework

Among various network models, U-Net stands out as the most widely used encoder–decoder model for medical image segmentation [28]. U-net is a neural network model that is usually used for medical image segmentation and its performance has become the baseline for most medical image semantic segmentation tasks. Fig. 5 below demonstrates the universal construction of a basic U-Net neural network [29]. It is proportion and contains two main portions: the compression (i.e. the encoder: left), and the expansion (i.e. the decoder: right). The compression part is a typical CNN structure, contain recurrent convolutions with a (3 × 3) kernel, followed by rectified linear unit (ReLU) operations and max pooling, and with each down-sampling procedure, there is a doubling of feature maps. At the end of each up-sampling, convolution is applied using a (3×3) kernel and a ReLU activation function. As a result of the up-sampling, new pixels are inserted between the existing ones, until the image reaches the wanted size. The final layer uses a 1×1 convolution, which schemes each feature vector onto the anticipated number of classes.

Thus, a Hybrid Framework of a U-net-based CNN style model is proposed for the diagnosis of AD. The core features of the U-net neural network comprise skip connections and a U-shaped structure with symmetrical encoders and decoders. The U-net executes down-sampling operations through the encoder to gain high-level semantic features and up-sampling operations through the decoder to correspondingly restore the high-level semantic feature map to the original image determination. At the same time, the network structure mixes the improved feature with the low-level features through skip connections, which helps the model not only learn the semantic features from MRI scans but also motivates the model to pay attention to the original subtle features. The classification of the images is performed using a hybrid approach, where texture features are learned by a custom U-Net-based CNN. The proposed hybrid framework U-Net-based CNN is applied based on the default U-Net architecture as shown in Fig. 6. It consists of ten layers:

1) Input Layer: Accepts pre-processed image data and texture features (GLCM) as inputs.
2) Down-sampling (encoding layer) involved 2 blocks,

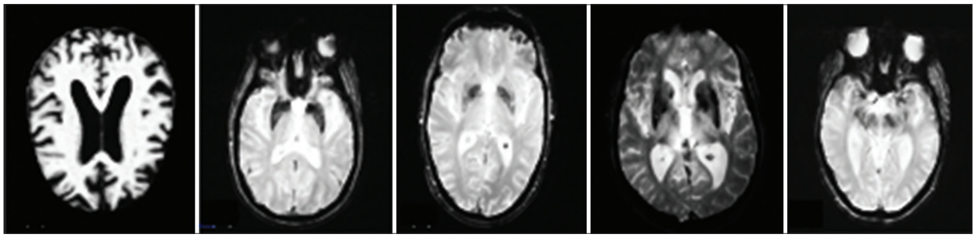

Fig. 3. The effect of applying CLAHE on the images and raising the contrast value.

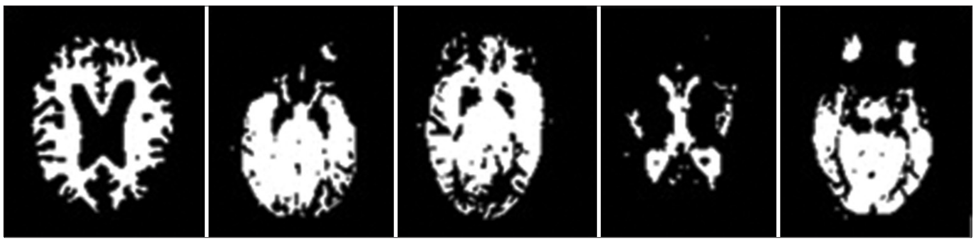

Fig. 4. Normalizing images to the range [0,1].

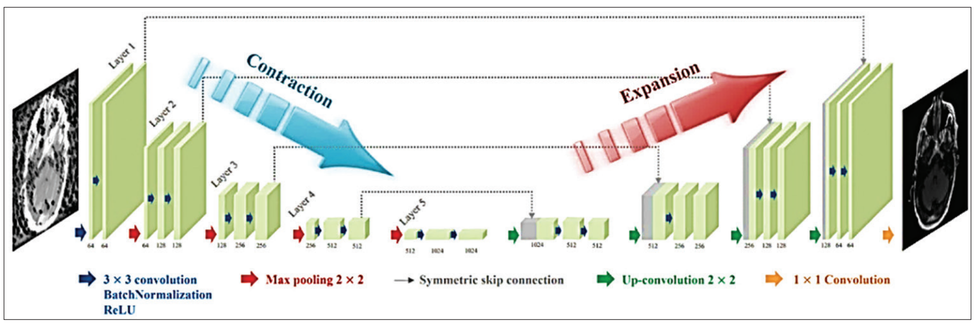

Fig. 5. U-shaped structure of the U-Net neural network [30].

and each block: Applied (conv2D (32) filters, kernel size = (3,3), activation= "ReLU", padding = "same") to reduce feature map dimensions by half and use Max-Pooling 2D (Pool size (2, 2), to reduces spatial dimensions.

3) Bottleneck layer to compress features to the smallest spatial representation Applied (conv2D: High-dimensional (128) filters and Dropout as a Regularization to reduce overfitting.
4) Up-sampling (decoding layer) with Size (2, 2) involved 2 blocks, and each block: Applied (Conv2D: 64 filters, kernel size (3, 3), padding = "same", Skip Connection: Concatenate with corresponding encoder block, Conv2D: 64 filters, kernel size (3, 3), padding = "same")
5) Fusion with GLCM features (Process GLCM texture features using a Dense layer (64 neurons), then combining processed GLCM features with the decoder output through concatenation.
6) Output layer, applied (conv2D layer with filters = number of classes and activation= "softmax" to produce class probabilities.
7) Compilation (loss function and optimizer) layer, involved: (a) Loss Function: categorical cross-entropy, multi-class classification, (b) Optimizer: Adaptive Moment Estimation optimizer, learning rate=$1e^{-4}$, (c) Metrics: Accuracy, Precision, Recall, and F1-score for performance evaluation.
8) Hybrid framework layer: combining spatial (U-Net-based) and texture (GLCM-based) features for classification, the objective was to leverage both spatial features (via CNN) and handcrafted descriptors (via GLCM) and the benefit was to improves classification by capturing complementary patterns, enhancing Alzheimer's detection accuracy.
9) Training the CNN: Pre-processed images and GLCM features are passed through the model, and Labels are one-hot encoded for multi-class support, then Train using augmented data (Techniques include rotation, shifting, and flipping) to improve generalization.
10) Optimization method: used Adaptive Moment Estimation

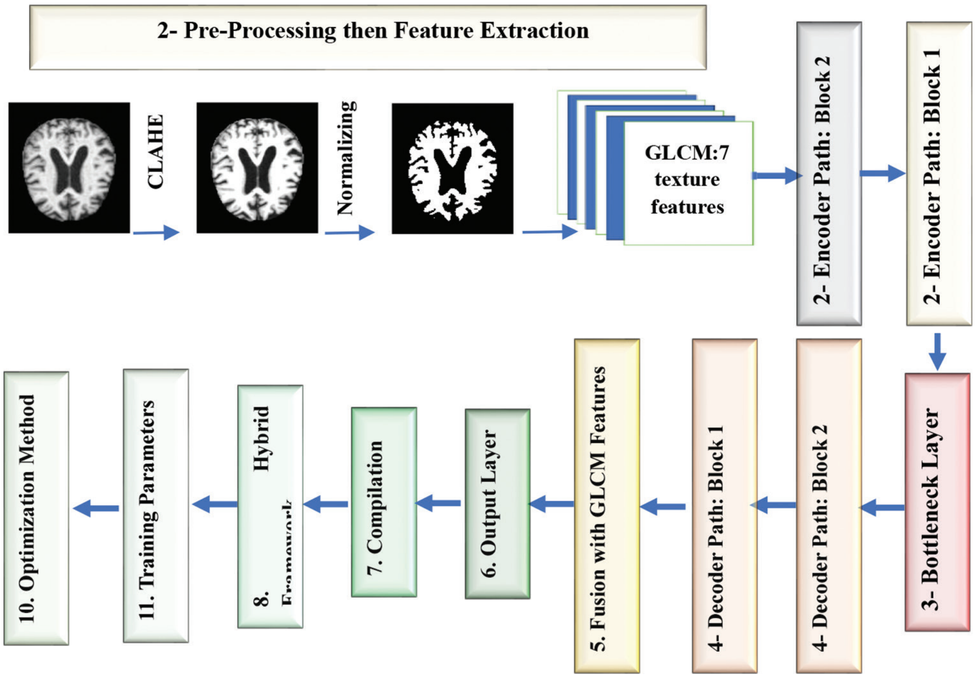

Fig. 6. The proposed hybrid framework U-Net-based convolutional neural network architecture.

optimizer (Adam) optimizer with adaptive learning rates to ensure smooth convergence during training.

11) Training parameters: Define epochs (20) and batch size (defined implicitly by the fit method) to balance speed and convergence.

3.4. Training Process for the Hybrid U-Net and CNN Model

The objective was to train the Hybrid U-Net with GLCM Features to learn spatial, texture-based, and semantic features for AD detection.

3.4.1. Inputs during training

a) Input Images: Pre-processed MRI scans fed into the U-Net encoder.
b) GLCM Features: Extracted texture features (contrast, homogeneity, energy, and correlation) concatenated at the decoder stage.
c) Labels: Ground truth labels (e.g., AD stages or healthy controls), either for segmentation maps (if using U-Net for segmentation) or for classification.

4. EXPERIMENTAL RESULT

4.1. Dataset

A Novel Image Casting and Fusion for Identifying deep Information utilized in this paper was gained from the ADNI information base (www.kaggle.com/datasets/kaushalsethia/alzheimers-adni) which is a comprehensive and widely used collection of MRI images format. ADNI inspires a direction for scientific researchers to main robust investigation and offer feasible evidence with different predictors around the world. The dataset contains a total of 18775 imaging sessions in which the patients or individuals are categorized into two groups (testing and Training) as shown in Table 2 below, and each group had alienated into five classes that are: AD, LMCI, MCI, EMCI, and CN.

TABLE 2: Total 18775 MRI images in ADNI classified into different AD categories

Groups	Classes	Testing images	Training images
Demented	AD	810	7536
	LMCI	72	72
	MCI	233	922
	EMCI	240	240
Non-Demented	CN	1220	7430
Total=18775		2575	16200

LMCI: Late mild cognitive impairment, MCI: Mild cognitive impairment, EMCI: Early mild cognitive impairment, CN: Cognitively normal, AD: Alzheimer's disease, MRI: Magnetic resonance imaging

4.2. Performance Metrics

a) Accuracy is the most common measure used to answer the question "Of all the predictions we made, how many were correct?," therefore ACC is the number of accurate predictions to the whole quantity of predictions. And calculated by Equation (1).

TABLE 3: CNN results without pre-processing

Groups	Classes	Accuracy (%)	Precision (%)	Recall (%)	F1-score (%)
Demented	AD	92.21	92.45	92.52	92.48
	LMCI	89.48	89.25	89.35	89.30
	MCI	90.41	90.74	91.74	91.24
	EMCI	90.85	90.35	91.40	90.87
Non-Demented	CN	93.98	93.48	92.11	92.79
Average		91.39	91.25	91.42	91.34

LMCI: Late mild cognitive impairment, MCI: Mild cognitive impairment, EMCI: Early mild cognitive impairment, CN: Cognitively normal, AD: Alzheimer's disease, CNN: Convolutional neural network

TABLE 4: CNN results after pre-processing

Groups	Classes	Accuracy (%)	Precision (%)	Recall (%)	F1-score (%)
Demented	AD	94.06	93.62	94.19	93.90
	LMCI	90.33	89.50	90.06	89.78
	MCI	90.66	90.59	91.84	91.21
	EMCI	91.80	91.51	92.15	91.83
Non-Demented	CN	93.83	93.33	91.96	92.64
Average		92.14	91.71	92.04	91.87

LMCI: Late mild cognitive impairment, MCI: Mild cognitive impairment, EMCI: Early mild cognitive impairment, CN: Cognitively normal, AD: Alzheimer's disease, CNN: Convolutional neural network

TABLE 5: U-Net model's performance after pre-processing

Groups	Classes	Accuracy (%)	Precision (%)	Recall (%)	F1-score (%)
Demented	AD	95.07	94.32	94.19	94.25
	LMCI	91.34	90.52	90.82	90.67
	MCI	91.58	92.61	92.06	92.33
	EMCI	93.55	92.12	92.28	92.20
Non-Demented	CN	93.83	93.33	91.96	92.64
Average		93.07	92.58	92.26	92.42

LMCI: Late mild cognitive impairment, MCI: Mild cognitive impairment, EMCI: Early mild cognitive impairment, CN: Cognitively normal, AD: Alzheimer's disease

TABLE 6: The final results from the five categories in the ADNI dataset using U-netbased CNN

Groups	Classes	Accuracy (%)	Precision (%)	Recall (%)	F1-score (%)
Demented	AD	96.08	96.32	96.39	96.35
	LMCI	92.35	92.12	92.22	92.17
	MCI	93.28	93.61	94.61	94.11
	EMCI	93.72	93.22	94.27	93.74
Non-Demented	CN	96.85	96.35	94.98	95.66
Average		94.46	94.32	94.49	94.41

LMCI: Late mild cognitive impairment, MCI: Mild cognitive impairment, EMCI: Early mild cognitive impairment, CN: Cognitively normal, AD: Alzheimer's disease, ADNI: Alzheimer's disease Neuroimaging Initiative, CNN: Convolutional neural network

TABLE 7: Comparative six models experimental results

Model	Accuracy (%)	Precision (%)	Recall (%)	F1-score (%)
FCN	93.71	93.52	94.30	93.91
SegNet	94.06	94.23	94.51	94.37
ResNet	93.41	94.12	93.97	94.04
DenseNet	94.14	94.09	93.66	93.87
U-Net	94.46	94.32	94.49	94.41%

$$Accuracy = \frac{TP + FP + TN + FN}{TP + FP + TN + FN} \times 100 \tag{1}$$

b) Precision is a metric that gives you the number of true positives to the number of total positives that the model expects. Or we can say "the obtainable of all the positive predictions we completed, how many were correct?", it is calculated by Equation (2).

TABLE 8: Accuracy rate of other approaches with the same ADNI dataset

Techniques	Accuracy (%)	Precision (%)	Recall (%)	F1-score (%)
Xia *et al*. 2020 [17]	94.19	-	-	-
Zhu *et al*. 2021 [19]	92.40	-	-	-
Shoaip *et al*. 2021 [20]	94.10	94.3	-	-
Helal *et al*. in 2022 [21]	94.34	-	-	-
Chen *et al*. 2023 [23]	87.83	87.83	92.66	87.83
Bhosale *et al*. 2023 [24]	91.23	-	-	-
Gupta *et al*. 2024 [2]	94.33	90.4	90.3	91.2
Firdos *et al*. in 2024 [25]	94			
Proposed Approach	94.46	94.32	94.49	94.41

$$Precision = \frac{TP}{TP + FP} \times 100 \quad (2)$$

c) Recall focuses on how good the model is at the outcome of all the positives. It is also entitled "true positive rate" and replies the question "Out of all the data points that should be predicted as true, how many did we acceptably predict as true?", Recall is calculated by Equation (3).

$$\text{Recall} = \frac{TP}{TP + FN} \times 100 \quad (3)$$

d) F1-score: Balances precision and recall, making it most useful when dealing with imbalanced datasets or unequal error costs, F1-score is calculated by Equation (4).

$$\text{Recall} = \frac{2 \times \text{ Recall} \times \text{Precision}}{\text{Recall} + \text{Precision}} \times 100 \quad (4)$$

4.3. Performance Evaluation

As a baseline DL method, we first assessed the CNN model without and then after pre-processing, the findings are shown in Tables 3 and 4.

Next, we evaluated the U-Net model's performance independently after pre-processing, as indicated in Table 5.

Finally, the hybrid approach, which combines CNN and U-Net, was then used to examine the possible advantages of this integration. Table 6 displays the final results for the four metrics are detailed with the final average for each metric for the five categories in the ADNI dataset.

4.4. Models Validation

To validate our technique and ensure the segmentation effect of the proposed hybrid U-Net framework model, other four models, including FCN, SegNet, Resnet, and Densenet were tested on the same prepared dataset, the results in Table 7 showed the strength of our proposed model.

4.5. Performance Comparison

More tests were conducted to evaluate our suggested technique's performance by comparing it with other techniques. Our suggested hybrid technique achieves the greatest performance (accuracy, precision, recall, and F1-score), as shown by the findings in Table 8. Some of certain cells are left blank since all of the most recent methods either tested their strategy only in terms of accuracy or combined accuracy with recall or F1-score.

5. CONCLUSION

Even though DL was initially successful in clinical practice, there are still difficulties in identifying complicated lesions and many intersecting diseases, which calls for the development of more DL-based approaches. When it comes to clinical intelligence-guided decision-making, these analytical endeavors include identifying barriers, creating prediction models, and other essential components that form the basis. The effectiveness of the U-net CNN model was demonstrated by obtaining final average results for the four measures: accuracy (94.46%), precision (94.32%), recall (94.49%), and F1-score (94.41%) as overall rates. The experiment results demonstrate that skip connections and deep supervision can improve the classification model's performance. The U-net CNN model was applied to RMI images from the ADNI dataset, which specializes in AD diagnosis.

REFERENCES

[1] A. Bhandarkar, P. Naik, K. Vakkund, S. Junjappanavar, S. Bakare and S. Pattar. "Deep learning based computer aided diagnosis of Alzheimer's disease: A snapshot of last 5 years, gaps, and future directions". Springer, Berlin, pp. 1-62, 2024.

[2] M. Gupta, R. Kumar and A. Abraham. "Adversarial network-based classification for Alzheimer's disease using multimodal brain images: A critical analysis". *IEEE Access*, Vol. 12, pp. 48366-48378, 2024.

[3] S. Mu, S. Shan, L. Li, S. Jing, R. Li, C. Zheng and X. Cui. "DMA-HPCNet: Dual Multi-level attention hybrid pyramid convolution neural network for Alzheimer's disease classification". *IEEE Access*, vol. 32, pp. 1955-1964, 2024.

[4] H. A. Helaly, M. Badawy and A. Y. Haikal. "Deep learning approach for early detection of Alzheimer's disease". *Cognitive Computation*, Vol. 14, pp. 711-1727, 2022.

[5] WHO. "*Dementia*". World Health Organization, 2023. Available from: https://www.who.int/health-topics/dementia#tab=tab_1 [Last accessed on 2024 Dec 02].

[6] A. A. Fakoya and Parkinson S. "A novel image casting and fusion for identifying individuals at risk of alzheimer's disease using MRI and PET Imaging". *IEEE Access*, Vol. 12, pp. 134101-134114, 2024.

[7] J. Silva, B. C. Bispo, P. M. Rodrigues and Alzheimer's Disease Neuroimaging Initiative. "Structural MRI texture analysis for detecting Alzheimer's disease". *Journal of Medical and Biological Engineering*, vol. 43, pp. 227-238, 2023.

[8] T. Mahmood, A. Rehman, T. Saba, L. Nadeem and S. A. O. Bahaj. "Recent advancements and future prospects in active deep learning for medical image segmentation and classification". *IEEE Access*, Vol. 11, pp. 113623-113652, 2023.

[9] S. A. Javid and M. M. Feghhi. "*Early Diagnosis of Alzheimer's Disease from MRI Images with Deep Learning Model*". IEEE, United States, pp. 1-7, 2024.

[10] R. G. Akindele, S. Adebayo, P. S. Kanda and M. Yu. "AlzhiNet: Traversing from 2DCNN to 3DCNN, towards early detection and diagnosis of Alzheimer's disease". *arxiv.org*, Vol. 60, no. 12, pp. 1-13, 2024.

[11] S. Y. Lu. "A short survey on computer-aided diagnosis of Alzheimer's disease: Unsupervised learning, transfer learning, and other machine learning methods". *Scilight, AI Medicine*, Vol. 1, pp. 1-8, 2023.

[12] S. Sadek and Z. F. Makki. "*A Review of AI Techniques Using MRI Brain Images for Alzheimer's Disease Detection*". IEEE, United States, pp. 76-82, 2023.

[13] B. Youssef, A. Alksas, A. Shalaby, A. Mahmoud, E. Bogaert, N. S. Algahmdi, A. Neubacher, S. Contractor, M. Ghazal, A. Elmaghraby and A. El-Baz. "Integrated deep learning and stochastic models for accurate segmentation of lung nodules from computed tomography images: A novel framework". *IEEE Access*, Vol. 11, pp. 99807-99821, 2023.

[14] R. Al-Amri, R. K. Murugesan, M. Man, A. F. Abdulateef, M. A. Al-Sharafi and A. A. Alkahtani. "Anomaly analysis of Alzheimer's disease in PET images using an unsupervised adversarial deep learning model". *Applied Sciences*, vol. 11, no. 5, pp. 1-17, 2021.

[15] R. Yousef, G. Gupta, N. Yousef and M. Khari. "A holistic overview of deep learning approach in medical imaging". *Multimedia Systems*, Vol. 28, pp. 881-914, 2022.

[16] I. Konovalenko, P. Maruschak, J. Brezinová, O. Prentkovskis and J. Brezina. "Research of U-Net-based CNN architectures for metal surface defect detection". *Machines*, Vol. 10, no. 5, pp. 1-19, 2022.

[17] Z. Xia, G. Yue, Y. Xu, C. Feng, M. Yang and T. Wang. "*A novel end-to-end hybrid Network for Alzheimer's disease detection using 3D CNN and 3D CLSTM*". United States: IEEE, pp. 1-13, 2020.

[18] S. Murugan, C. Venkatesan, M. G. Sumithra, X. Z. Gao, B. Elakkiya, M. Akila and S. Manoharan. "Demnet: A deep learning model for early diagnosis of Alzheimer diseases and dementia from MR images". *IEEE Access*, vol. 9, pp. 90319-90329, 2021.

[19] W. Zhu, L. Sun, J. Huang, L. Han and D. Zhang. "*Dual attention multi-instance deep learning for Alzheimer's disease diagnosis with structural MRI*". IEEE, United States, Vol. 40, no. 9, p. 2354-2366, 2021.

[20] N. Shoaip, A. Rezk, S. El-Sappagh, T. Abuhmed, S. Barakat and M. Elmogy. "Alzheimer's disease diagnosis based on a semantic rule-based modeling and reasoning approach". *Computers, Materials and Continua CMC*, Vol. 9, pp. 3531-3548, 2021.

[21] H. A. Helaly, M. Badawy and A. Y. Haikal. "Toward deep MRI segmentation for Alzheimer's disease detection". *Neural Computing and Applications*, Vol. 34, pp. 1047-1063, 2022.

[22] J. H. Noh, J. H. Kim and H. D. Yang. "Classification of Alzheimer's progression using fMRI data". *Sensors* (*Basel*). Vol. 23, no. 14, pp. 1-14, 2023.

[23] X. Chen, B. Lei, C. M. Pun and S. Wang. "*Brain Diffuser: An End-to-end Brain Image to Brain Network Pipeline*". Springer Nature, Germany, pp. 16-26, 2023.

[24] T. Bhosale, M. Gulame, B. Shendkar, P. Kadam, R. More and R. Mali. "Alzheimer's Disease MRI Image Segmentation Based on the Enhanced U-Net". In: *IEEE, International Conference on ICT in Business Industry and Government (ICTBIG)*, pp. 1-5, 2023.

[25] S. M. Firdos, M. Z. Mehack, S. A. Muskan, A. BibiNadeefa and S. Kamepalli. "Enhancing Alzheimer's Disease Prediction Through Deep Learning Models: A Comparative study of GoogLeNet, LeNet, and UNet". In: *First International Conference on Innovations in Communications, Electrical and Computer Engineering (ICICEC)*, IEEE, 2024.

[26] P. K. Pandey, J. Pruthi, S. Alzahrani, A. Verma and B. Zohra. "Enhancing healthcare recommendation: Transfer learning in deep convolutional neural networks for Alzheimer disease detection". *Front* (*Lausanne*), Vol. 11, pp. 1-12, 2024.

[27] S. U. Khan, N. Islam, Z. Jan, K. Haseeb, S. I. A. Shah and M. Hanif. "A machine learning-based approach for the segmentation and classification of malignant cells in breast cytology images using gray level co-occurrence matrix (GLCM) and support vector machine (SVM)". *Neural Computing and Applications*, vol. 34, pp. 8365-8372, 2022.

[28] Y. Yuan and Y. Cheng. "Medical image segmentation with UNet-based multi-scale context fusion". *Scientific Reports*, Vol. 14, pp. 15687, 2024.

[29] S. H. Kang and Y. Lee. "Motion artifact reduction using U-net model with three-dimensional simulation-based datasets for brain magnetic resonance images". *Bioengineering* (*Basel*), Vol. 11, no. 3, pp. 227, 2024.